

Principal Component Analysis (PCA)-based Massive-MIMO Channel Feedback

Jingon Joung, Ernest Kurniawan, and Sumei Sun

Abstract—Channel-state-information (CSI) feedback methods are considered, especially for massive or very large-scale multiple-input multiple-output (MIMO) systems. To extract essential information from the CSI without redundancy that arises from the highly correlated antennas, a receiver transforms (sparsifies) a correlated CSI vector to an uncorrelated sparse CSI vector by using a Karhunen-Loève transform (KLT) matrix that consists of the eigen vectors of covariance matrix (CM) of CSI vector and feeds back the essential components of the sparse CSI, i.e., a principal component analysis method. A transmitter then recovers the original CSI through the inverse transformation of the feedback vector. Herein, to obtain the CM at transceiver, we derive analytically the CM of spatially correlated Rayleigh fading channels based on its statistics including transmit antennas' and receive antennas' correlation matrices, channel variance, and channel delay profile. With the knowledge of the channel statistics, the transceiver can readily obtain the CM and KLT matrix. Compression feedback error and bit-error-rate performance of the proposed method are analyzed. Numerical results verify that the proposed method is promising, which reduces significantly the feedback overhead of the massive-MIMO systems with marginal performance degradation from full-CSI feedback (e.g., feedback amount reduction by 80%, i.e., $\frac{1}{5}$ of original CSI, with spectral efficiency reduction by only 2%). Furthermore, we show numerically that, for a given limited feedback amount, we can find the optimal number of transmit antennas to achieve the largest spectral efficiency, which is a new design framework.

Index Terms—Channel feedback, massive (large-scale) MIMO, principal component analysis, Karhunen-Loève transform, channel state information compression.

I. INTRODUCTION

In communications, channel state information (CSI) can be used at a transmitter (Tx) to improve a quality-of-service (QoS). The CSI at the Tx (CSIT) enables a preprocessing at the Tx to overcome a poor channel condition incurring severe performance degradation. Especially, preprocessing techniques using multiple transmit antennas, such as a single user multiple-input multiple-output (MIMO) beamforming and a multiuser (MU) MIMO precoding (see [2]–[7] and references therein), are typical, promising methods for high-QoS communications systems.

The CSIT can be typically realized either by uplink (from receiver (Rx) to Tx) channel estimation at a Tx in time-division duplex (TDD) systems, e.g., implicit feedback in IEEE 802.11n [8], or by CSI feedback from an Rx to a Tx in frequency-division duplex (FDD) systems, e.g., explicit feedback in 802.11ac [9]. Phase calibration improves the

reciprocity between uplink and downlink (from Tx to Rx) TDD channels, so that the Tx can obtain the downlink CSI from the uplink CSI estimates [10]. On the other hand, channel feedback of FDD systems has a fundamental issue on the channel feedback overhead against the limited uplink channel capacity. Especially, when the number of antennas is very large, possibly a few tens or hundreds of antennas [11], [12], i.e., a massive or very large-scale MIMO, the channel feedback overhead issue becomes more severe and it renders the closed-loop feedback approach impractical. Hence, network throughput improvement cannot be guaranteed due to the uplink overhead even if the downlink throughput is improved [13].

For a conventional MIMO system with usually less than 10 antennas, reduced feedback information has been rigorously studied, such as a codebook (see [14] and references therein), channel distribution [15], partial CSI [16], and implicit CSI (e.g., rank, precoding matrix, and channel quality indicators) in [7]. However, it is difficult to directly apply the schemes to a massive MIMO system. For example, the codebook in general requires high computational complexity, even for the case of eight transmit antennas [17]. The high complexity design issue also persists in a random vector quantization (RVQ) approach for the codebook generation. Hence, a reduced size of codebook can be considered for the systems. However, due to the very large dimension of the massive MIMO channels, this approach will degrade the communication performance severely [18], and the optimal finite-size codebook design for the very large dimension arises as a new issue. Another issue related to method is the scalability for an MU massive MIMO scenario. The massive MIMO may not embrace the optimality of MU-MIMO codebook from single-user MIMO codebook, e.g., the 3rd generation partnership project long-term evolution Release-8 MU-MIMO codebook to reduce the channel feedback amount, we may consider distributing the many antennas and feeding back only the local CSI for strong channels instead of the global CSI including weak channels [19]. As a directly possible way for collocated massive MIMO systems, CSI (or equivalent antennas) grouping is proposed [20], [21]. As demonstrated in [21], correlation due to the many collocated antennas within the limited space of massive MIMO Tx and Rx imposes redundancy on CSI information and it makes possible that the amount of feedback can be significantly reduced by grouping the highly correlated CSIs, although the best grouping pattern and the total number of groups are yet to be analyzed further [20].

In this work, we consider *compressive channel feedback* using a sparse *principal component analysis* (PCA) technique,

Part of this work has been published in Proceedings of the IEEE Globecom 2014, Austin, TX, USA, December 2014 [1].

The authors are with the Institute for Infocomm Research (I²R), A*STAR, Singapore 138632 (e-mail: {jgjong, ekurniawan, sunsm}@i2r.a-star.edu.sg)

and propose a sparse channel feedback (SCF) method based on the PCA for massive MIMO systems. The PCA is a well established tool for various applications, such as genetics, chemistry, meteorology, image processing, machine learning, and data mining, to reduce high dimensional data to a smaller dimension by also exploiting the correlation in the data. Precisely, the PCA extracts M principal components that are uncorrelated from N correlated components ($N \gg M$) by using signal transformation [22], [23], i.e., a dimensionality reduction of a set with correlated components. For the transformation, the PCA employs optimal transformation using a Karhunen-Loève transform (KLT) matrix that consists of eigen vectors of a CSI covariance matrix such that the original CSI can be compressed efficiently with no correlation¹ [24]–[27]. The Tx can recover the original CSI by inverse-transforming the sparse CSI with the KLT matrix based on a compressive sampling/sensing (CS) theory [25], [28], [29]. Notwithstanding the optimality of the KLT in terms of the compression, it is challenging to employ the KLT in the channel feedback due to the data/signal-dependent characteristic of the KLT matrix. Introducing alternative methods, such as an adaptive algorithm² [25], [27] and an empirical method [26], we derive a closed form expression of the *covariance matrix* of spatially correlated Rayleigh fading channels, which consists of transmit and receive *correlation matrices*, channel *variance*, and channel *delay profile*. The tractable representation of the channel covariance matrix enables the implementation of PCA-based channel feedback and provides analytical tradeoff between data compression and communication performance, i.e., a normalized mean-squared error (NMSE). Numerical results verify that the proposed SCF method can improve a compression performance, i.e., increase a compression ratio sustaining communication performance. For example, feedback amount can be reduced by 68% with no spectral efficiency loss and it can be reduced by 80%, i.e., 1/5 amount of original CSI, with spectral efficiency reduction by only 2%. Furthermore, the SCF method can have lower implementation complexity and, in practice, could be more stable and robust as compared to the instantaneous channel feedback schemes. At last, we justify that the proposed SCF method using KLT is a promising channel feedback method for the massive MIMO systems by answering for one possible question “Why do not we just reduce the number of transmit antennas and feed back the full CSI without compression?”

The rest of the paper is organized as follows. In Section II, channel feedback and compressive sampling are briefly introduced. In Section III, we propose an SCF method using PCA. Section IV provides error analysis on compressive feedback. Simulation results are shown in Section V. Section VI concludes the paper.

Notations: $\|\mathbf{a}\|_p$ represents p -norm of vector \mathbf{a} ; \mathbf{A}^{-1} , \mathbf{A}^\dagger , \mathbf{A}^T and \mathbf{A}^H are the inverse, pseudoinverse, transpose, and

Hermitian transpose of \mathbf{A} , respectively; \mathbf{I}_a and $\mathbf{0}_{a,b}$ are a -dimensional identity matrix and an a -by- b zero matrix, respectively.

II. CSI FEEDBACK AND COMPRESSIVE SAMPLING

We first introduce the model of channel feedback, and briefly recapitulate the basic of compressive sampling/sensing (CS) to interpret the channel feedback method from CS perspective. The interpretation of channel feedback based on CS will help us to understand the sparse-domain channels and the sparse channel feedback (SCF) mechanism, and to capture the essential part of the proposed SCF in Section III.

A. CSI Feedback

Let a channel vector be $\mathbf{h} \in \mathbb{C}^{N \times 1}$ that consists of spatial- and-frequency domain N channel elements and is supposed to be fed back to a Tx. When we compress N samples of \mathbf{h} to M samples, where $M \leq N$, a data (information) compression ratio is defined for given N as

$$1 \leq \gamma(M) \triangleq N/M < \infty.$$

In this study, we consider a *compressive feedback error* that arises only from the compression not from estimation at an Rx and Tx. In other words, we assume that an Rx can estimate and feed back the compressed information of \mathbf{h} perfectly, and a Tx can also obtain the compressed M feedback samples without distortion. Hence, the discrepancy between the recovered channels $\tilde{\mathbf{h}}$ at the Tx and the original channel \mathbf{h} may exist only if $\gamma(M) > 1$, and it is quantitatively measured by a normalized mean-squared error (NMSE) $\delta(M)$, i.e., a compressive feedback error, defined as

$$0 \leq \delta(M) \triangleq \mathbb{E} \|\mathbf{h} - \tilde{\mathbf{h}}\|_2^2 / \mathbb{E} \|\mathbf{h}\|_2^2 < \infty. \quad (1)$$

We will derive $\delta(M)$ analytically in Section IV.

Larger $\gamma(M)$ and smaller $\delta(M)$ are desired for *efficient* (i.e., less feedback overhead sustaining performance) and *reliable* (i.e., less performance degradation) communications. Typically, there is a tradeoff between the efficiency and the reliability in communications (or tradeoff between interpretability and statistical fidelity in data acquisition [23]). In other words, if M decreases (or increases), both compression ratio $\gamma(M)$ and NMSE $\delta(M)$ increases (or decreases). However, the tradeoff may disappear depending on the channel characteristics. For example, we can increase $\gamma(M)$ sustaining the $\delta(M)$ if $\mathbf{h} = [h \cdots h]^T$. In that case, a Tx can achieve a zero NMSE from feedback of only h for any γ . Note that the basic assumption in the example is that the Tx knows that the channel is *static*. The lesson from the example is that the knowledge of the channel statistics, such as correlation information in the example, can be used to reduce CSI, which inspires us to consider an SCF method based on CS.

B. Compressive Sampling/Sensing (CS)

The CS is a technique to recover N original samples (i.e., \mathbf{h}) from its compressed $M < N$ observation samples (i.e., $\mathbf{y} \in \mathbb{C}^{M \times 1}$) [25], [28], [29]. To extract the effective

¹Note that PCA exploits the correlation information between CSIs to reduce the feedback amount, yet it achieves the compression by representing the CSI vector in terms of its dominant eigen spaces instead of grouping the CSI with similar values as in [20].

²Recently, in [27], a tracking algorithm for channel’s principal component is proposed by tracking a perturbation term of CSI.

information from \mathbf{h} and to construct an observation vector \mathbf{y} , a *measurement* matrix $\Phi \in \mathbb{C}^{M \times N}$ is used as $\mathbf{y} = \Phi \mathbf{h}$. Now, the CS forms ℓ_1 minimization problem as

$$\tilde{\mathbf{s}} = \underset{\mathbf{s} \in \mathbb{R}^{N \times 1}}{\text{minimize}} \|\mathbf{s}\|_1, \text{ s.t. } \mathbf{y} = \Phi \mathbf{h} = \Phi \Psi^{-1} \mathbf{s} \quad (2)$$

where \mathbf{s} is the sparse representation of the original signal such that

$$\mathbf{s} = \Psi \mathbf{h}, \quad (3)$$

and $\Psi \in \mathbb{C}^{N \times N}$ is a *representation* matrix. Linear programming can be used to find the sparse signal \mathbf{s} for given \mathbf{y} , Φ , and Ψ in (2). Once $\tilde{\mathbf{s}}$ is obtained from (2), \mathbf{h} can be recovered as

$$\tilde{\mathbf{h}} = \Psi^{-1} \tilde{\mathbf{s}}. \quad (4)$$

A robust uncertainty principle in [28] states that the number of minimum required observation samples, M , for the perfect recovery of \mathbf{s} in (2) is reduced as the \mathbf{s} becomes more sparse. Concretely, for the perfect recovery of K -sparse \mathbf{s} that includes K -nonzero and $(N - K)$ -zero elements, the number of observation samples M should fulfill $M \geq cK \ln N$, where $c > 0$ a small constant. Herein, note that the sparsity K depends on the representation matrix Ψ in (3).

C. Interpretation of channel feedback from a CS Perspective

When we consider CS for channel feedback in communications, along with the recovery performance, we have to consider the feedback amount, which is an overhead in communications. Therefore, contrary to the CS in data processing, in which the original \mathbf{h} is recovered from the observation $\mathbf{y} \in \mathbb{C}^{M \times 1}$, the channel feedback in communications feeds back the K -sparse signal $\mathbf{s} \in \mathbb{C}^{K \times 1}$ to recover \mathbf{h} because $K < M$, i.e.,

$\text{CS: } \mathbf{y} \text{ (} M \text{ observations)} \xrightarrow{\ell_1 \text{ minimization}} \tilde{\mathbf{h}} \text{ (} N \text{ data recovery)}$
$\text{channel feedback: } \mathbf{s} \text{ (} K\text{-sparse repr.)} \xrightarrow{M \text{ feedback}} \tilde{\mathbf{h}} \text{ (} N \text{ channel recovery)}$

A feedback amount is assumed to be fixed to avoid additional overhead to inform it. Hence, regardless of the sparsity of \mathbf{s} , the Rx feeds back M samples from \mathbf{s} by using a selection matrix $\mathbf{S} \in \mathbb{R}^{M \times N}$ that is a binary matrix to select the most significant feedback information from \mathbf{s} . Each row of \mathbf{S} selects one sparse channel. Precisely, the n th element is ‘1’ and other elements in the row are ‘0’s if the n th element of \mathbf{s} is selected to be fed back. Since each element of \mathbf{s} could be selected at most once, each column of \mathbf{S} includes at most one ‘1’.

The Rx feeds back the selected sparse CSI vector \mathbf{s}' to a Tx, where \mathbf{s}' is written as $\mathbf{s}' = \mathbf{S} \mathbf{s} \in \mathbb{C}^{M \times 1}$, and a Tx recovers the channels from \mathbf{s}' based on (3) and (4) as follows:

$$\tilde{\mathbf{h}} = \Psi^{-1} \mathbf{S}^\dagger \mathbf{s}' = \Psi^{-1} \mathbf{S}^\dagger \mathbf{S} \mathbf{s} = \Psi^{-1} \mathbf{S}^\dagger \mathbf{S} \Psi \mathbf{h}. \quad (5)$$

In (5), if $M \geq K$, we can design \mathbf{S} such that $\mathbf{S}^\dagger \mathbf{S} \mathbf{s} = \overline{\mathbf{I}}_M \mathbf{s} = \mathbf{s}$, where $\overline{\mathbf{I}}_M$ is a diagonal matrix whose diagonal element is either 1 or 0, and K of M non-zero diagonal

elements correspond to the non-zero elements of \mathbf{s} . As consequence, the Tx can recover \mathbf{h} perfectly. Note that, contrary to the CS, a measurement matrix Φ and an ℓ_1 minimization are not required for channel feedback and the recovery, and that the design of Ψ and \mathbf{S} is a critical part affecting the channel recovery performance in channel feedback.

1) *Design of Ψ* : The main purpose of a representation matrix Ψ is to transform \mathbf{h} as sparse as possible, so that K and also M can be reduced without any loss of information. To this end, the representation matrix Ψ can be designed based on the *channel characteristics*. For example, there are various well-known transforms, such as the discrete Fourier/sine/cosine/Hartley transform (DFT/DST/DCT/DHT) and KLT, depending on the channel characteristics. If \mathbf{h} itself is sufficiently sparse, we can set Ψ to an identity matrix \mathbf{I}_N . If the \mathbf{h} is quasi-static (looks like a step function), a difference matrix $\text{Tz}[[1, -1, 0, \dots, 0]^T]$ will best sparsify \mathbf{h} , where $\text{Tz}[\mathbf{a}]$ generates a Toeplitz matrix with \mathbf{a} as its first row vector. A DFT matrix can be used to capture the frequency-domain correlated channels. The DST/DCT has good energy compaction property; thus, it can achieve near-optimal compression performance. However, DST/DCT does not perform very well if the channels are highly correlated [24]. As mentioned in Introduction, a PCA using KLT is an optimal transform that can decorrelate the channels into a representation with the most sparse, non-redundant channels. In Section III, we design the KLT matrix from channel statistics, such as spatial correlation, variance, and delay profile of \mathbf{h} .

2) *Design of \mathbf{S}* : After transforming the original channel \mathbf{h} to \mathbf{s} , the selection matrix \mathbf{S} can be designed according to the *sparsity characteristics* of \mathbf{s} . For example, if the sparse channels are distributed randomly over the sparse domain, \mathbf{S} is designed to select the significant, sparse channels. In the case, along with the sparse channel values, the Rx needs to feed back the index of the selected channels, i.e., selection matrix \mathbf{S} is a variable, which requires $\log_2 \prod_{m=0}^{M-1} (N - m)$ additional feedback bits per dimension to inform the index of ‘1’ of each of M rows. On the other hand, if the significant channels are typically located within a fixed sparse-domain regime, i.e., \mathbf{s} is structured sparsity, \mathbf{S} can be fixed to be implemented at both Tx and Rx.

III. PROPOSED SPARSE CSI FEEDBACK

Based on PCA, we have a representation matrix Ψ that consists of eigenvectors of channel covariance matrix as [22], [23], [30]

$$\overline{\Psi} = \text{eig} \left(\mathbf{C}_h \triangleq \text{E}(\mathbf{h}\mathbf{h}^H) \right) \in \mathbb{C}^{N \times N}, \quad (6)$$

where $\text{eig}(\mathbf{A})$ takes \mathbf{U}^H from an eigenvalue decomposition such that $\mathbf{A} = \mathbf{U}\mathbf{D}\mathbf{U}^H$. Here, \mathbf{D} is a diagonal matrix whose diagonal elements are the eigenvalues of \mathbf{A} , and \mathbf{U} ’s column vectors are the eigenvectors of \mathbf{A} . The PCA designs a selection matrix \mathbf{S}_{PCA} such that it selects the M largest eigen values of $\overline{\Psi}$. Hence, the most significant sparse channels will be selected. In a practical communications system, however, it is challenging to obtain the exact \mathbf{C}_h , which motivates us to

represent the channel covariance matrix C_h with respect to the tractable channel statistics of \mathbf{h} .

To derive C_h analytically, following Property 1 regarding a CSI structure is useful.

Property 1: The CSI structure of \mathbf{h} does not affect the CSI recovery performance in an SCF scheme. In other words, a restructured CSI with an arbitrary permutation matrix $\mathbf{P} \in \mathbb{R}^{N \times N}$, i.e., $\mathbf{P}\mathbf{h}$, provides the same recovery performance as the original \mathbf{h} in an SCF scheme.

Proof: See Appendix B. \blacksquare

Using the Property 1, without loss of generality, we structure a *spatial-and-frequency* domain channel vector \mathbf{h} as follows:

$$\mathbf{h} = \text{vec}([\mathbf{h}_1 \cdots \mathbf{h}_{N_f}]) = [\mathbf{h}_1^T \cdots \mathbf{h}_{N_f}^T]^T \in \mathbb{C}^{N \times 1}, \quad (7)$$

where $\text{vec}(\mathbf{A})$ denotes a vectorization of a m -by- n matrix \mathbf{A} to form the mn -by-1 column vector obtained by stacking the columns of the matrix \mathbf{A} on top of one another; N_f is the number of subbands (subcarriers); \mathbf{h}_n is the spatial-domain channel vector for frequency band n that is modeled as

$$\mathbf{h}_n = \text{vec}(\mathbf{H}(n)) \in \mathbb{C}^{N_r N_t \times 1}, \quad n \in \{1, \dots, N_f\};$$

$\mathbf{H}(n) \in \mathbb{C}^{N_r \times N_t}$ is the spatially correlated MIMO channel matrix of subcarrier n ; N_r and N_t are number of receive and transmit antennas; and $N = N_r N_t N_f$. The spatially correlated MIMO channel is represented by [31]

$$\mathbf{H}(n) = \mathbf{R}_r^{\frac{1}{2}} \mathbf{H}_{\text{iid}}(n) \left(\mathbf{R}_t^{\frac{1}{2}} \right)^H,$$

where $\mathbf{R}_r \in \mathbb{R}^{N_r \times N_r}$ and $\mathbf{R}_t \in \mathbb{R}^{N_t \times N_t}$ are receive- and transmit-antenna correlation matrices, respectively (for a spatial correlation model of 2-dimension antenna, see Appendix A), and $\mathbf{H}_{\text{iid}}(n) \in \mathbb{C}^{N_r \times N_t}$ is the uncorrelated, spatial-domain MIMO channel matrix of subcarrier n . The (i, j) th elements of $\mathbf{H}_{\text{iid}}(n)$ represents a channel gain consisting of the path loss and the small scale fading between transmit antenna j and receive antenna i . The channel elements are assumed to obey the complex normal distribution with a zero mean and a σ_h^2 variance, i.e., $\mathcal{CN}(0, \sigma_h^2)$, and be independent and identically distributed (i.i.d.).

The channel structure in (7) allows us to derive the closed form of C_h as shown in Property 2.

Property 2: For the channel vector \mathbf{h} , whose structure follows (7), its covariance matrix is derived formally as

$$\mathbf{C}_h = \mathbf{C}_f \otimes (\mathbf{R}_t \otimes \mathbf{R}_r),$$

where \otimes represents Kronecker product of two matrices; $\mathbf{C}_f = \text{Tz}[c_1^2, \dots, c_{N_f}^2]$ is a frequency-domain covariance matrix; and c_n^2 is the correlation factor between the frequency domain channels $\mathbf{H}_{\text{iid}}(1)$ and $\mathbf{H}_{\text{iid}}(n)$. For the frequency domain channels generated by DFT of L -tap time domain channels with a delay profile $\mathbf{d} \in \mathbb{R}^{L \times 1}$, the correlation factor c_n^2 is expressed as

$$c_n^2 = \sigma_h^2 \text{tr} \left(\mathbf{f}_1^{r,H} \mathbf{f}_n^r \text{diag}(\mathbf{d}) \right), \quad \forall n \in \mathcal{N} = \{1, \dots, N_f\}.$$

Here, $\mathbf{f}_n^r \in \mathbb{C}^{1 \times L}$ is the n th row vector of $\mathbf{F}_L \in \mathbb{C}^{N \times L}$ that consists of the first L column vectors of N -point DFT matrix $\mathbf{F} \in \mathbb{C}^{N \times N}$.

Proof: See Appendix C for the proof. \blacksquare

Algorithm 1 : Sparse CSI Feedback (SCF)

1) Offline/Online Mode: Setup

- a) measure the required channel statistics, namely σ_h^2 , \mathbf{d} , \mathbf{R}_t , and \mathbf{R}_r .
- b) compute C_h from Property 2.
- c) using C_h , compute $\bar{\Psi}$ in (6).
- d) store $\bar{\Psi}$ at both Tx and Rx.

2) Rx's: Feedback from each Rx, $\mathbf{S} = \mathbf{S}_{\text{KLT}}(M)$

- a) estimate channels $\mathbf{H}(n)$ for all $n = \{1, \dots, N_f\}$.
- b) construct \mathbf{h} in (7).
- c) get a sparse channel representation $\mathbf{s} = \bar{\Psi} \mathbf{h}$.
- d) generate a selected sparse vectors $\mathbf{s}' = \mathbf{S} \mathbf{s}$.
- e) feed back \mathbf{s}' , and \mathbf{S} if it is needed.

3) Tx: Recovery at Tx from (5)

- a) recover the channels as $\tilde{\mathbf{h}} = \bar{\Psi}^{-1} \mathbf{S}^\dagger \mathbf{s}'$.
-

Remark 1: The representation matrix $\bar{\Psi}$ is fixed at both Tx and Rx and no additional eigen decomposition and feedback are required, especially, when the Rx is nomadic and thus the covariance matrix C_h is static [32]. Only the M -selected sparse channels, \mathbf{s}' , need to be fed back for CSI recovery at a Tx.

Remark 2: The time variation of channel statistics is caused by the movement of a Rx, hence the offline estimates may be outdated and are needed to be updated by feedback. Depending on Rx mobility, each Rx measures the channel variance delay profile and feeds back them to a Tx, so that the Tx can update $\bar{\Psi}$. The sporadic update of the statistics can dramatically reduce the feedback information compared to the update of $\bar{\Psi}$ itself, and it alleviates the high overhead feedback and Rx complexity issues.

Remark 3: One alternative implementation of C_h in (6) is an empirical cumulative moving average as $\tilde{C}_h \triangleq \frac{1}{t} \sum_{t'=1}^{t'=t} \{\mathbf{h}_{t'} \mathbf{h}_{t'}^H\} \in \mathbb{C}^{N \times N}$, where t is update time [26]. By updating every T interval, feedback amount can be reduced. However, after \tilde{C}_h is numerically evaluated at an Rx, the new KLT matrix $\bar{\Psi}$ should be updated at both Tx and Rx. Since the Rx has to compute the \tilde{C}_h and recalculate $\bar{\Psi}$, the computational complexity may arise as an issue at the Rx that has insufficient computing capability. Furthermore, the update of $\bar{\Psi}$ still requires channel feedback overhead.

IV. COMPRESSIVE FEEDBACK ERROR ANALYSIS

The quality of the channel recovery depends on the level of compression. The channel recovery error is expected to be more severe when the compression ratio $\gamma(M)$ is high, while it decreases as $\gamma(M)$ decreases. In practical systems, it is often necessary to give a performance guarantee to the users. In such cases, a quantitative analysis on the tradeoff between the compression ratio and the channel recovery performance is useful, since it specifies the constraint on how much compression can be tolerated for a given QoS requirement.

Following the discussion in Section II, the compressive feedback error is considered solely from the compression, and

does not include the estimation and quantization errors. The NMSE in (1) is calculated using \mathbf{h} in (7) and $\tilde{\mathbf{h}}$ in Algorithm 1. In the proposed SCF using KLT, the amount of feedback (and correspondingly the compression ratio) is determined by the number of non-zero elements in the selection matrix \mathbf{S} . Without compression ($\gamma(M) = 1$), the amount of feedback would be equal to $N = N_r N_t N_f$ (the dimension of \mathbf{h}). In reality, due to correlation in frequency and spatial domain of the antennas, the actual number of dimension occupied by \mathbf{h} is usually less than N . Considering that any realization of \mathbf{h} can be expressed as $\mathbf{h} = \mathbf{C}_h^{1/2} \mathbf{a}$ where $\mathbf{a} \sim \mathcal{C}(0, \mathbf{I}_N)$, the number of non-zero elements N' in \mathbf{a} required to fully represent \mathbf{h} is the same as the rank of \mathbf{C}_h , i.e., $\text{rank}(\mathbf{C}_h)$. From the fact that we can achieve $\delta(M) = 0$ when $N' \geq \text{rank}(\mathbf{C}_h)$, a maximum distortion-free compression ratio denoted by γ^* is derived as

$$\gamma^* = \frac{N}{\text{rank}(\mathbf{C}_h)} = \frac{N_f}{\underbrace{\text{rank}(\mathbf{R}_f)}_{\triangleq \gamma_f}} \frac{N_t}{\underbrace{\text{rank}(\mathbf{R}_t)}_{\triangleq \gamma_t}} \frac{N_r}{\underbrace{\text{rank}(\mathbf{R}_r)}_{\triangleq \gamma_r}} \triangleq \gamma_f \gamma_t \gamma_r \quad (8)$$

The result in (8) is obtained by choosing the selection matrix \mathbf{S} to extract components of $\text{eig}(\mathbf{C}_h)$ corresponding to the non-zero $M = N'$ eigenvalues and by using Property 2. An interesting remark from (8) is as follows.

Remark 4: The maximum distortion-free compression ratio γ^* is the product of the individual distortion-less compression ratio at each of the domains, i.e., $\gamma^* = \gamma_f \gamma_t \gamma_r$ where γ_f , γ_t , and γ_r are at the frequencies, transmit antennas, and receive antennas, respectively. Therefore, the effect of low rank CMs and the corresponding magnitude of the distortion-less compression ratios will be more pronounced when the correlation is present in multiple domains due to the multiplying effect as concretely shown in (8).

When higher compression ratio is desired, some of the components of \mathbf{s} in (5) corresponding to the non-zero eigenvalues have to be discarded as well, resulting in the recovery distortion. As described in the earlier section, following the idea of PCA, the best selection strategy is to discard the elements that correspond to the smallest eigenvalue first. Denoting the number of principle components that are kept as $M < N'$, the NMSE $\delta(M)$ is derived as (see Appendix D)

$$\delta(M) = \frac{\sum \text{uncaptured } (N' - M) \text{ principal components}}{\sum \text{all } N' \text{ principal components}} \quad (9)$$

The NMSE $\delta(M)$ can be interpreted as the *best possible distortion* for a given compression ratio of $\gamma = N/M$, and it is also known as a *distortion of data recovery* in the CS context [28]. In other interpretation, the minimum number of principal components to be kept for a given compression ratio γ is given by $M = N/\gamma$, and the selection matrix \mathbf{S} will contain M non-zero components. The resulting NMSE $\delta(M)$ can then be calculated using (9). We can also use (9) in system design when allocating the feedback bandwidth for a given QoS constraint, e.g., NMSE and bit-error-rate (BER).

Now, we analyze the system performance in terms of the BER to get the answer how the choice of compression ratio $\gamma(M)$ affects the BER performance. Assuming that beamforming is used at both the spatial and frequency dimension, and

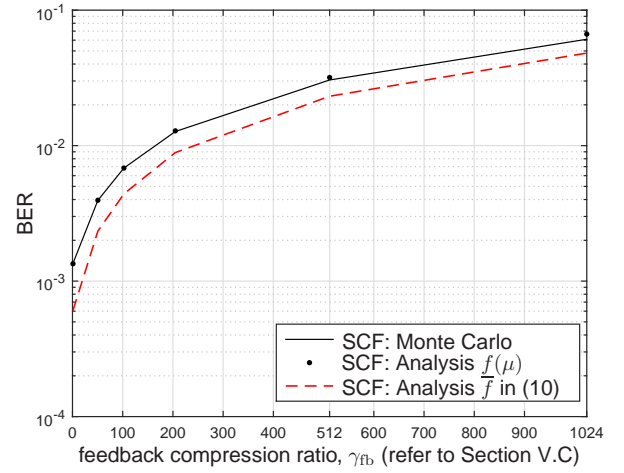


Fig. 1. BER evaluation and BER analysis justification.

using the fact that the subspace of the channel estimation error and that of the channel estimate are orthogonal to one another, we can derive an effective signal-to-noise ratio, denoted by μ , as $\mu = \|\tilde{\mathbf{h}}\|^2/\sigma^2$, where $\tilde{\mathbf{h}}$ is the reconstructed channel vector and σ^2 is the noise variance. With μ , the BER can then be derived as a convex function of μ ; for example, $f(\mu) = 3/4\mathcal{Q}(\sqrt{\mu/5}) + 1/2\mathcal{Q}(\sqrt{3\mu/5}) - 1/4\mathcal{Q}(\sqrt{\mu})$ for 16-QAM modulation with Gray bit mapping [33], where $\mathcal{Q}(x) = \int_x^\infty (2\pi)^{-0.5} \exp(-0.5t^2) dt$ is a standard Q-function. By the convexity of the Q-function and invoking Jensen's inequality, the lower bound on the average BER \bar{f} can then be obtained as follows (refer to the notation in Appendix D):

$$\begin{aligned} \bar{f} &\triangleq \mathbb{E}_{\tilde{\mathbf{h}}} (f(\mu)) \geq f(\mathbb{E}[\mu]) = f\left(\sigma^{-2} \text{tr}\left(\mathbb{E}\left(\tilde{\mathbf{h}}\tilde{\mathbf{h}}^H\right)\right)\right) \\ &= f\left(\sigma^{-2} \text{tr}\left(\mathbf{C}_h^{1/2} \mathbf{S}^\dagger \mathbf{S} \mathbb{E}(\mathbf{a}\mathbf{a}^H) (\mathbf{S}^\dagger \mathbf{S})^H \mathbf{C}_h^{1/2}\right)\right) \\ &= f\left(\sigma^{-2} \text{tr}(\mathbf{S}\mathbf{D})\right) = f\left(\sigma^{-2} \text{tr}(\mathbf{D})(1 - \delta(M))\right). \end{aligned} \quad (10)$$

From (10), we can clearly see the relationship between the effect of compression ratio $\delta(M)$ on the BER performance \bar{f} .

For the verification of the BER and NMSE analyses, please refer to Fig. 1 and Fig. 2(a). The BER (16-QAM) is evaluated for a single user using beamforming $\tilde{\mathbf{h}}^H$, when $N_{t,h} = 64$, $N_{t,v} = 1$, $N_r = 1$, and $N_f = 64$, i.e., $N = 2^{12} = 4096$.

V. PERFORMANCE EVALUATION AND DISCUSSION

With the analytical framework proposed in the earlier sections, we further verify the proposed SCF method by comparing it with other channel feedback schemes summarized in Table I. We consider OFDM system and compare basically three schemes, namely, frequency-domain channel feedback, time-domain channel feedback, and the proposed SCF using $\tilde{\Psi}$, which are denoted by FCF, TCF, and SCF, respectively, with the suffixes 'f' and 'v' for fixed and variable \mathbf{S} , respectively. To clearly compare the performance, all comparison results are obtained for fixed σ_h^2 and \mathbf{d} . After briefly introducing the FCF and TCF, we show the comparison results. For the fixed \mathbf{S}_{PCA} we fix it by $\mathbf{S}_{\text{PCA}}(M) \triangleq [\mathbf{I}_M \mathbf{0}_{M,N-M+1}]$.

TABLE I
CSI FEEDBACK (FB) SCHEMES WITH $\gamma = N/M$ AND Q -BIT QUANTIZATION.

Schemes	Ψ	S	FB info.	Total number of FB bits	CSI structure	Acronym
Freq-domain CSI FB	I_N	$S_{\text{FCF}}(M)$	s'	$2MQ$	\mathbf{h} in (7)	FCF-f1
					\mathbf{h}' in (13)	FCF-f2
Time-domain CSI FB	F^{-1}	$S_{\text{TCF}}(M)$	s'	$2MQ$	\mathbf{h} in (7)	TCF-f1
					\mathbf{h}' in (13)	TCF-f2
		variable	S and s'	$2MQ + 2 \log_2 \prod_{m=0}^{M-1} (N-m)$	\mathbf{h} in (7)	TCF-v1
Sparse-domain CSI FB	$\tilde{\Psi}$	$S_{\text{PCA}}(M)$	s'	$2MQ$	\mathbf{h} in (7)	SCF-f
		variable	S and s'	$2MQ + 2 \log_2 \prod_{m=0}^{M-1} (N-m)$		SCF-v
Full CSI FB	-	-	\mathbf{h}	$2NQ$ (no compression)	-	Full channel feedback

A. Frequency-domain CSI Feedback (FCF)

For the sake of comparison, an identity matrix I_N is employed as a representation matrix. The identity representation matrix gives us the simplest way that reduces the feedback information by feeding back the partially, directly selected information from the original channel \mathbf{h} as follows:

$$s' = S_{\text{FCF}} \mathbf{s} = S_{\text{FCF}} I_N \mathbf{h} = S_{\text{FCF}} \mathbf{h}, \quad (11)$$

where S_{FCF} is a selection matrix. Since the original channel \mathbf{h} is the aggregation of frequency-domain spatial channels, we call this scheme as a FCF methods. Having the knowledge of predetermined S_{FCF} and feedback information s' , the Tx can obtain the estimate of the original channels as follows:

$$\tilde{\mathbf{h}} = \text{intp} \left(S_{\text{FCF}}^\dagger s' \right), \quad (12)$$

where $\text{intp}(\cdot)$ represents an interpolation function to recover the unselected channels in (11). The recovery performance of FCF depends on the interpolation method, the selection matrix, and the original channel structure³. Designing the interpolator and selection matrix is out of the scope of this work. For the channel structure, we consider another structure defined as

$$\mathbf{h}' = \text{vec} \left([\mathbf{h}_1 \cdots \mathbf{h}_{N_f}]^T \right), \quad (13)$$

which is similar to the bundled channel structure in [34].

In simulation, we fix the selection matrix of FCF by S_{FCF} that selects the channels located in equidistance of frequency domain axis to feed back. For the interpolation, we employ a spline interpolation method [35]. As mentioned, since an optimal selection matrix depends on the interpolation method and channel distribution, we do not consider a variable selection matrix for the FCF. Though the FCF method requires low computational complexity at the transceiver, the compression ratio γ is generally desired to be low to achieve reliable CSI recovery performance in communications.

B. Time-domain CSI Feedback (TCF)

An inverse DFT (IDFT) matrix F^{-1} is employed as a representation matrix. Since the Rx feeds back the IDFT of the aggregation of frequency-and-spatial domain channels, for simple denotation, we address this scheme as a TCF method.

³Contrary of the SCF method, in which the channel structure does not affect the CSI recovery performance as shown in Property 1, the channel structure generally affects on the recovery performance.

Fixed and variable selection matrices are considered for the TCF method. The fixed selection matrix is designed to capture the most significant channels from \mathbf{s} . In simulation, we fix the selection matrix as $S_{\text{TCF}} = \begin{bmatrix} I_{M/2} & \mathbf{0}_{M/2, N-M/2+1} \\ \mathbf{0}_{M/2, N-M/2+1} & I_{M/2} \end{bmatrix}$ to capture the most significant time-domain channels from \mathbf{h}' . The variable selection matrix selects the most significant M elements in \mathbf{s} .

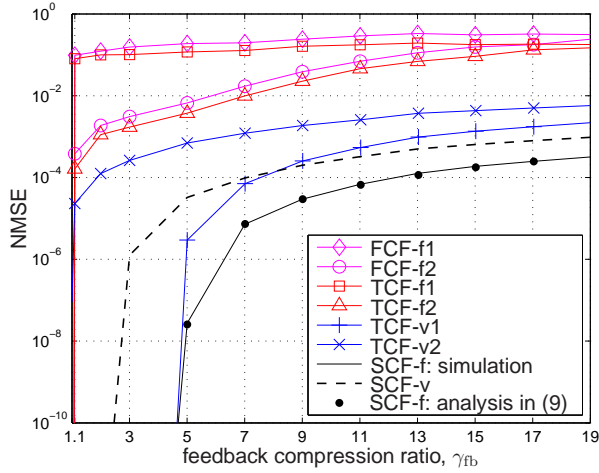
Compared to the FCF method, the CSI recovery of TDF does not require interpolation, yet it requires re-transformation, i.e., DFT, to recover the CSI at the Tx, which is the same as the procedure in (5). The recovery performance depends on the selection method and the sparsity of \mathbf{s} . Since the IDFT and DFT are already implemented in the OFDM transceiver, and thus the TCF method is natural to be considered for the channel feedback of OFDM systems.

C. Simulation Results

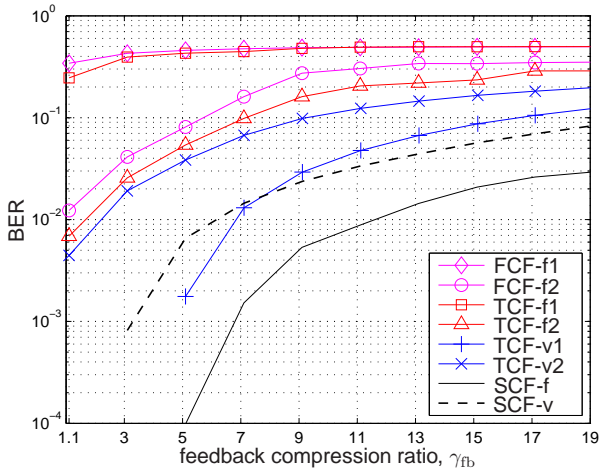
The number of feedback bits for real and imaginary values of each scheme is summarized at the fifth column in Table I when the data compression ratio is fixed by $\gamma = N/M$ and Q -bit quantization is employed. Since the different schemes generally require different numbers of feedback bits, we define a *feedback compression ratio* as

$$\gamma_{\text{fb}} = \frac{\text{Total number of feedback bits without compression}}{\text{Total number of feedback bits with compression}}$$

and fairly compare the performances for the same γ_{fb} . For the performance metric, we consider channel recovery performance at Tx and communications performance at Rx, namely an NMSE and a BER (16-QAM). We consider one Tx and four Rx's, i.e., an MU massive MIMO system. The Tx and each Rx have 64 and two 2-D antennas with the configuration of $N_t = 64$ ($N_{t,h} = N_{t,v} = 8$) and $N_r = 2$ ($N_{r,h} = 2$, $N_{r,v} = 1$). The Tx is located at the center of 1km-by-1km square-shaped coverage. Four Rx's are uniformly located within the coverage in each channel realization, and the corresponding large-scale fading is set into the variance σ_h^2 of the uncorrelated Rayleigh fading channels accordingly. The path loss model follows that $-123 + 10 \log_{10}(l^{-3.76})$, where l is distance between Tx and Rx in kilometer. Channel delay follows an exponential decaying profile and the number of channel taps is seven, i.e., $L = 7$. Tx and Rx antenna spatial correlation factors are $\rho_t = 0.8$ and $\rho_r = 0.5$, respectively. All Rx's share 64 subcarriers, i.e., $N_f = 64$, and feed back their own CSI, individually and independently. 12 bits are used for



(a)



(b)

Fig. 2. Performance comparison over feedback compression ratio γ_{fb} . (a) NMSE at Tx. (b) BER at Rx.

the quantization of the feedback symbols, i.e., $Q = 12$. The Tx supports multiple Rx's by using a zero-forcing-based MU-MIMO precoding, which can be obtained from the aggregated CSIs. System bandwidth is 10 MHz and maximum transmit power is 43 dBm and noise variance at the Rx is set to be -174 dBm/Hz.

In Figs. 2(a) and (b), the NMSE and BER (averaged over four Rx's) are shown, respectively. From the results, we see that the communication performance BER is directly affected by the CSI recovery performance, i.e., NMSE, because the MU interferences increases as the CSI uncertainty increases. We observe the agreement between the NMSE analysis in (9) and the numerical result. The channel recovery performance of FCF-f1 is very poor. This is because the variation of channel elements of \mathbf{h} in (7) is significant, so that the interpolator cannot recover the original channels. The serious degradation of interpolation performance can be mitigated by structuring the original channels to \mathbf{h}' in (13), i.e., FCF-f2. On the other hand, the performance of TCF-f1 is also very poor as the channels after IDFT of \mathbf{h} are distributed randomly over the time domain. Hence, the fixed selection matrix \mathbf{S}_{TCF} does

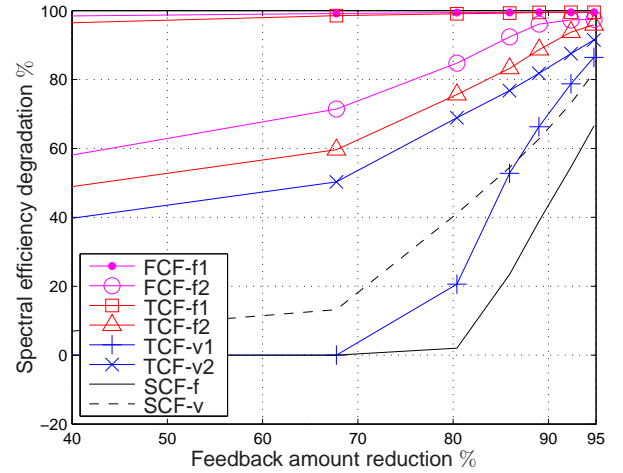


Fig. 3. Spectral efficiency reduction over feedback amount reduction.

not capture the significant channels, resulting in huge loss of information. Similar to FCF, restructuring \mathbf{h} to \mathbf{h}' can improve TCF performance as shown with TCF-f2. Herein, the significant time-domain channels are located most likely at the boundary of the time domain, which are well aligned to \mathbf{S}_{TCF} . Further performance improvement can be achieved by selecting the channels according to their strength with allowing the additional feedback for the variable selection matrix, namely TCF-v1 and TCF-v2. From one interesting result that TCF-v1 outperforms TCF-v2, we see that the time-domain channel of \mathbf{h} is more sparse than that of \mathbf{h}' . Contrary of TCF, in which the variable selection improves the performance effectively, for the proposed SCF, additional feedback for a variable selection matrix does not improve the performance. In other words, fortunately, the sparse-domain channels are mainly located within specific range that corresponds to the fixed selection matrix \mathbf{S}_{KLT} . Since the channels' sparsity is high and their distribution are sufficiently captured by \mathbf{S}_{KLT} already, the additional feedback decreases the compression performance. Up to $\gamma_{fb} = 4$, no compression errors arise for TCF-v1 and SCF-f and, thus, which is the same as the optimal BER with perfect CSI, i.e., a Full channel feedback. The compression performance improvement through the proposed SCF is significant. For example, to achieve 0.03 BER performance, the SCF-f can reduce the feedback information around by half compared to the TCF-v1, i.e., from $\gamma_{fb} = 9$ to $\gamma_{fb} = 19$. The numerical results verify that the proposed SCF-f achieves always the best compression performance with the smallest NMSE and BER for given γ_{fb} , i.e., for given feedback amount.

In Fig. 3, we evaluate spectral efficiency (SE) degradation from a SE bound, which is obtained from Full channel feedback. The SE is defined by the sum of each user's throughput $\log_2(1 + \text{SINR})$. The SE reduction of each scheme is shown over feedback amount reduction, i.e., $(\gamma_{fb} - 1)/\gamma_{fb} \times 100$ %. From the results, we can quantify how much the communication performance degrades due to the compression of each FB scheme. For example, TCF-v2 achieves SE that is degraded from its bound by 20% with 80% feedback amount reduction,

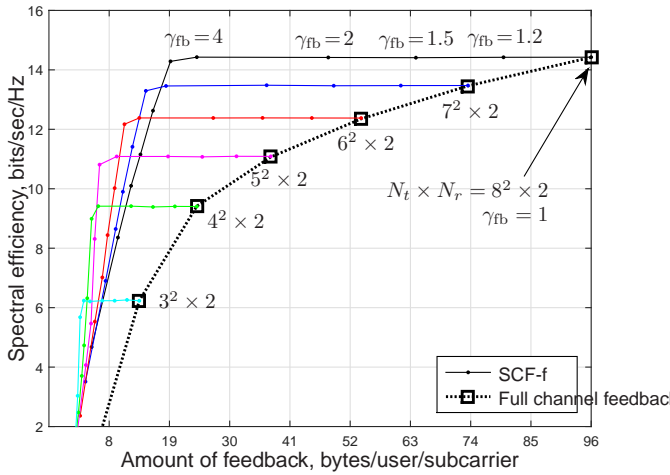


Fig. 4. Spectral efficiency comparison over feedback amount.

yet the proposed SCF-f can achieve near optimal performance with feedback amount reduction up to 80% (SE reduction by 2% with feedback amount reduction by 80%). As shown, the SE of the proposed SCF-f achieves the best SE regardless of the feedback amount reduction. One interesting observation is that we can still communicate with 95%-reduced CSI information, even though the SE is degraded by about 65%. Such a reduced SE could be one possible application for low-rate transmission, e.g., control signal from data collection center to distributed multiple sensors in sensor networks.

In Fig. 4, we evaluate the SE's of the proposed SCF-f scheme for various $N_t = a^2$ ($N_{t,v} = a$ and $N_{t,h} = a$) over the actual amount of feedback bytes. Square marks represent SEs with full channel feedback. As we increase a feedback compression ratio γ_{fb} , the actual amount of feedback bytes (value in x-axis) decreases, while SE (value in y-axis) is retained up to a certain level of γ_{fb} and then to decrease. The results verify that always the proposed SCF-f can reduce feedback amount without performance compromise. From the results, interestingly, we can observe that the maximum SE at given feedback amount is obtained not necessarily from larger number of N_t . For example, if the feedback amount is limited by 8 bytes/user/subcarrier due to the uplink capacity, the best choice of N_t is 25 rather than 36, 49, and 64. This particular observation provides important message to us that we have to consider the uplink capacity limitation to maximize downlink SE in the communications systems with feedback.

VI. CONCLUSION

We have considered a compression method to feed back CSI for large-scale MIMO systems. A covariance matrix of spatially correlated Rayleigh fading channels has been analytically modeled and used to sparsify the original CSI based on PCA. From intensive performance evaluation of NMSE, BER, and SE, we have justified that the proposed sparse CSI feedback method can reduce the CSI amount significantly and effectively.

APPENDIX A 2-DIMENSIONAL SPATIAL CORRELATION

Consider a rectangular shape of transmit antenna arrays. Suppose that the minimum distance of adjacent antennas is δ . The antenna index is allocated from top-left antenna to bottom-right antenna, i.e., Zig-Zag. Similarly, we index the receive antennas. Following the antenna indices, we first construct an uncorrelated, spatial-domain MIMO channel matrix $\mathbf{H}_{iid}(n) \in \mathbb{C}^{N_r \times N_t}$. The correlation is then simply characterized by correlation factors ρ_t and ρ_r . The factors ρ_t and ρ_r represent the correlation strength between the adjacent antennas separated by δ at the transmitter and receiver, respectively. Using ρ_t and ρ_r and the fact that spatial correlation is inversely proportional to the distance δ between antennas [31], the \mathbf{R}_r and \mathbf{R}_t of the 2-D antennas can be modeled as follows:

$$\begin{aligned} \mathbf{R}_t &= \text{BlkTz}[\mathbf{T}_1, \dots, \mathbf{T}_{N_{t,v}}] \in \mathbb{R}^{N_t \times N_t} \\ \mathbf{R}_r &= \text{BlkTz}[\mathbf{T}'_1, \dots, \mathbf{T}'_{N_{r,v}}] \in \mathbb{R}^{N_r \times N_r}, \end{aligned}$$

where \mathbf{T}_m and \mathbf{T}'_m are defined at (A.1) at the bottom of next page; and $\text{BlkTz}[\mathbf{A}_1, \dots, \mathbf{A}_N]$ and $\text{Tz}[a_1, \dots, a_N]$ produce a symmetric block Toeplitz and Toeplitz matrices as

$$\begin{bmatrix} \mathbf{A}_1 & \dots & \mathbf{A}_N \\ \vdots & \ddots & \vdots \\ \mathbf{A}_N & \dots & \mathbf{A}_1 \end{bmatrix} \text{ and } \begin{bmatrix} a_1 & \dots & a_N \\ \vdots & \ddots & \vdots \\ a_N & \dots & a_1 \end{bmatrix},$$

respectively.

APPENDIX B PROOF OF PROPERTY 1

Suppose that the covariance matrix of the original channels is decomposed as $\mathbf{E}(\mathbf{h}\mathbf{h}^H) = \mathbf{U}\mathbf{D}\mathbf{U}^H$. Let the new channel structure with an arbitrary permutation matrix \mathbf{P} be $\mathbf{h}' = \mathbf{P}\mathbf{h}$. Then the new covariance matrix of the new CSI vector is derived as

$$\begin{aligned} \mathbf{E}(\mathbf{h}'(\mathbf{h}')^H) &= \mathbf{E}(\mathbf{P}\mathbf{h}\mathbf{h}^H\mathbf{P}^H) = \mathbf{P}\mathbf{E}(\mathbf{h}\mathbf{h}^H)\mathbf{P}^H \\ &= \mathbf{P}\mathbf{U}\mathbf{D}\mathbf{U}^H\mathbf{P}^H. \end{aligned} \quad (\text{B.1})$$

From (B.1), we get the new KLT matrix as $\overline{\Psi}' = (\mathbf{P}\mathbf{U})^H$. Now, using the new KLT matrix, we get the new sparse channel vector $\mathbf{s}' = \overline{\Psi}'\mathbf{h}'$. From the property of the permutation matrix that $\mathbf{P}^H = \mathbf{P}^{-1}$, we get $\mathbf{s}' = (\mathbf{P}\mathbf{U})^H\mathbf{h}' = (\mathbf{P}\mathbf{U})^H\mathbf{P}\mathbf{h} = \mathbf{U}^H\mathbf{h}$, and can show that the new sparse channels are uncorrelated as follows:

$$\mathbf{E}(\mathbf{s}'(\mathbf{s}')^H) = \mathbf{U}^H \mathbf{E}(\mathbf{h}\mathbf{h}^H) \mathbf{U} = \mathbf{U}^H \mathbf{U} \mathbf{D} \mathbf{U}^H \mathbf{U} = \mathbf{D},$$

which implies that the same CSI recovery performance will be achieved regardless of \mathbf{P} .

APPENDIX C PROOF OF PROPERTY 2

Proof: Let express the spatial correlation matrices and the uncorrelated channel matrix as follows: $\mathbf{R}_r^{\frac{1}{2}} = [\mathbf{r}_1 \dots \mathbf{r}_{N_r}]$; $\mathbf{R}_t^{\frac{1}{2}} = [\mathbf{t}_1 \dots \mathbf{t}_{N_t}]$; and $\mathbf{H}_{iid}(n) = [(\mathbf{h}_1^i(n))^T \dots (\mathbf{h}_{N_r}^i(n))^T]^T$, where $\mathbf{r}_i \in \mathbb{R}^{N_r \times 1}$ and $\mathbf{t}_i \in \mathbb{R}^{N_t \times 1}$ are the i th column vectors of $\mathbf{R}_r^{\frac{1}{2}}$ and $\mathbf{R}_t^{\frac{1}{2}}$, respectively, and

$\mathbf{h}_j^r(n) \in \mathbb{C}^{N_t \times 1}$ is the j th row vector of $\mathbf{H}_{\text{iid}}(n)$. Then, we can express the channel vector of the n th subcarrier as

$$\mathbf{h}_n = \left[\left(\sum_{i=1}^{N_r} (\mathbf{r}_i \mathbf{h}_i^r(n)) \mathbf{t}_1 \right)^T \cdots \left(\sum_{i=1}^{N_r} (\mathbf{r}_i \mathbf{h}_i^r(n)) \mathbf{t}_{N_t} \right)^T \right]^T,$$

and derive the cross correlation matrix between the subcarrier n and n' as (C.1) at the bottom of this page. Herein, $c_{nn'}^2 = \mathbb{E} \left(\sum_{i=1}^{N_r} \mathbf{h}_i^r(n) \mathbf{h}_i^{r,H}(n') \right) / (N_r N_t)$ is the correlation of the channels of frequency n and n' . In (C.1), (a) follows since $\mathbf{h}_i^r(n)$ and $\mathbf{h}_j^r(n')$ are uncorrelated if $i \neq j$, $\forall n, n' \in \{1, \dots, N_f\}$, (b) follows from the independence of all elements of $\mathbf{h}_i^r(n)$, so that $\mathbb{E} \left(\mathbf{h}_i^r(n) \mathbf{t}_a \mathbf{t}_b^H \mathbf{h}_i^{r,H}(n') \right) = c_{nn'}^2 \text{tr}(\mathbf{t}_a \mathbf{t}_b^H) = c_{nn'}^2 \mathbf{t}_b^H \mathbf{t}_a$. Using (C.1), the covariance matrix of the channel is simply rewritten as (C.2) at the bottom of this page.

channels, we derive $c_{nn'}^2$ as follows:

$$\begin{aligned} c_{nn'}^2 &= \frac{1}{N_r N_t} \mathbb{E} \left(\sum_{i=1}^{N_r} \mathbf{h}_i^r(n) \mathbf{h}_i^{r,H}(n') \right) \\ &= \mathbb{E} \left(\left[\mathbf{F}_L(\mathbf{h}_{r,t} \odot \sqrt{\mathbf{d}}) \right]_n \left[\mathbf{F}_L(\mathbf{h}_{r,t} \odot \sqrt{\mathbf{d}}) \right]_{n'}^* \right) \\ &= \mathbb{E} \left(\mathbf{f}_n^r(\mathbf{h}_{r,t} \odot \sqrt{\mathbf{d}}) \left(\sqrt{\mathbf{d}^H} \odot \mathbf{h}_{r,t}^H \right) \mathbf{f}_{n'}^{r,H} \right) \\ &= \text{tr} \left(\mathbf{f}_{n'}^{r,H} \mathbf{f}_n^r \mathbb{E} \left(\mathbf{h}_{r,t} \odot \sqrt{\mathbf{d}} \sqrt{\mathbf{d}^H} \odot \mathbf{h}_{r,t}^H \right) \right) \\ &= \text{tr} \left(\mathbf{f}_{n'}^{r,H} \mathbf{f}_n^r \text{diag}(\mathbf{d}) \sigma_h^2 \right), \end{aligned}$$

where $\mathbf{h}_{r,t} \in \mathbb{C}^{L \times 1}$ is L -by-1 complex normal distributed random variable, i.e., $\mathbf{h}_{r,t} \sim \mathcal{CN}(0, 1)$, for realizing the time domain channels from transmit antenna t to the receive antenna r ; \odot represents the elementwise product; and $[\mathbf{a}]_n$ and $[\mathbf{a}]_n^*$ are the n th element of a vector \mathbf{a} and its complex conjugate, respectively. Since $\mathbf{f}_{n'}^{r,H} \mathbf{f}_n^r = \mathbf{f}_{n_1}^{r,H} \mathbf{f}_{n_2}^r$ for any n_1 and n_2 such that $|n_2 - n_1| = |n' - n|$, by denoting $c_n^2 = c_{1n}^2$, we can simply rewrite the first term in (C.2) as follows:

$$\begin{bmatrix} c_{11}^2 & \cdots & c_{1N_f}^2 \\ \vdots & \ddots & \vdots \\ c_{N_f 1}^2 & \cdots & c_{N_f N_f}^2 \end{bmatrix} = \text{Tz}[c_1^2, \dots, c_{N_f}^2],$$

where $c_n^2 = \sigma_h^2 \text{tr} \left(\mathbf{f}_1^{r,H} \mathbf{f}_n^r \text{diag}(\mathbf{d}) \right)$. This completes the

Now, based on the definition of the frequency domain

$$\begin{aligned} \mathbf{T}_m &= \text{Tz} \left[\rho_t \sqrt{(m-1)^2 + 0^2}, \rho_t \sqrt{(m-1)^2 + 1^2}, \dots, \rho_t \sqrt{(m-1)^2 + N_{t,h}^2} \right] \in \mathbb{R}^{N_{t,h} \times N_{t,h}} \\ \mathbf{T}'_m &= \text{Tz} \left[\rho_r \sqrt{(m-1)^2 + 0^2}, \rho_r \sqrt{(m-1)^2 + 1^2}, \dots, \rho_r \sqrt{(m-1)^2 + N_{r,h}^2} \right] \in \mathbb{R}^{N_{r,h} \times N_{r,h}}. \end{aligned} \quad (\text{A.1})$$

$$\begin{aligned} \mathbb{E}(\mathbf{h}_n \mathbf{h}_{n'}^H) &= \begin{bmatrix} \mathbb{E} \left(\sum_{i=1}^{N_r} (\mathbf{r}_i \mathbf{h}_i^r(n)) \mathbf{t}_1 \mathbf{t}_1^H \sum_{i=1}^{N_r} (\mathbf{h}_i^{r,H}(n') \mathbf{r}_i^H) \right) & \cdots & \mathbb{E} \left(\sum_{i=1}^{N_r} (\mathbf{r}_i \mathbf{h}_i^r(n)) \mathbf{t}_1 \mathbf{t}_{N_t}^H \sum_{i=1}^{N_r} (\mathbf{h}_i^{r,H}(n') \mathbf{r}_i^H) \right) \\ \vdots & \ddots & \vdots \\ \mathbb{E} \left(\sum_{i=1}^{N_r} (\mathbf{r}_i \mathbf{h}_i^r(n)) \mathbf{t}_{N_t} \mathbf{t}_1^H \sum_{i=1}^{N_r} (\mathbf{h}_i^{r,H}(n') \mathbf{r}_i^H) \right) & \cdots & \mathbb{E} \left(\sum_{i=1}^{N_r} (\mathbf{r}_i \mathbf{h}_i^r(n)) \mathbf{t}_{N_t} \mathbf{t}_{N_t}^H \sum_{i=1}^{N_r} (\mathbf{h}_i^{r,H}(n') \mathbf{r}_i^H) \right) \end{bmatrix} \\ &\stackrel{(a)}{=} \begin{bmatrix} \mathbb{E} \left(\sum_{i=1}^{N_r} (\mathbf{r}_i \mathbf{h}_i^r(n) \mathbf{t}_1 \mathbf{t}_1^H \mathbf{h}_i^{r,H}(n') \mathbf{r}_i^H) \right) & \cdots & \mathbb{E} \left(\sum_{i=1}^{N_r} (\mathbf{r}_i \mathbf{h}_i^r(n) \mathbf{t}_1 \mathbf{t}_{N_t}^H \mathbf{h}_i^{r,H}(n') \mathbf{r}_i^H) \right) \\ \vdots & \ddots & \vdots \\ \mathbb{E} \left(\sum_{i=1}^{N_r} (\mathbf{r}_i \mathbf{h}_i^r(n) \mathbf{t}_{N_t} \mathbf{t}_1^H \mathbf{h}_i^{r,H}(n') \mathbf{r}_i^H) \right) & \cdots & \mathbb{E} \left(\sum_{i=1}^{N_r} (\mathbf{r}_i \mathbf{h}_i^r(n) \mathbf{t}_{N_t} \mathbf{t}_{N_t}^H \mathbf{h}_i^{r,H}(n') \mathbf{r}_i^H) \right) \end{bmatrix} \\ &\stackrel{(b)}{=} \begin{bmatrix} c_{nn'}^2 \mathbf{t}_1^H \mathbf{t}_1 \sum_{i=1}^{N_r} (\mathbf{r}_i \mathbf{r}_i^H) & \cdots & c_{nn'}^2 \mathbf{t}_{N_t}^H \mathbf{t}_1 \sum_{i=1}^{N_r} (\mathbf{r}_i \mathbf{r}_i^H) \\ \vdots & \ddots & \vdots \\ c_{nn'}^2 \mathbf{t}_1^H \mathbf{t}_{N_t} \sum_{i=1}^{N_r} (\mathbf{r}_i \mathbf{r}_i^H) & \cdots & c_{nn'}^2 \mathbf{t}_{N_t}^H \mathbf{t}_{N_t} \sum_{i=1}^{N_r} (\mathbf{r}_i \mathbf{r}_i^H) \end{bmatrix} = c_{nn'}^2 \begin{bmatrix} \mathbf{t}_1^H \mathbf{t}_1 & \cdots & \mathbf{t}_{N_t}^H \mathbf{t}_1 \\ \vdots & \ddots & \vdots \\ \mathbf{t}_1^H \mathbf{t}_{N_t} & \cdots & \mathbf{t}_{N_t}^H \mathbf{t}_{N_t} \end{bmatrix} \otimes \sum_{i=1}^{N_r} (\mathbf{r}_i \mathbf{r}_i^H) \\ &= c_{nn'}^2 (\mathbf{R}_t) \otimes (\mathbf{R}_r) \end{aligned} \quad (\text{C.1})$$

$$\mathbb{E}(\mathbf{h} \mathbf{h}^H) = \begin{bmatrix} \mathbb{E}(\mathbf{h}_1 \mathbf{h}_1^H) & \cdots & \mathbb{E}(\mathbf{h}_1 \mathbf{h}_{N_f}^H) \\ \vdots & \ddots & \vdots \\ \mathbb{E}(\mathbf{h}_{N_f} \mathbf{h}_1^H) & \cdots & \mathbb{E}(\mathbf{h}_{N_f} \mathbf{h}_{N_f}^H) \end{bmatrix} = \begin{bmatrix} c_{11}^2 (\mathbf{R}_t) \otimes (\mathbf{R}_r) & \cdots & c_{1N_f}^2 (\mathbf{R}_t) \otimes (\mathbf{R}_r) \\ \vdots & \ddots & \vdots \\ c_{N_f 1}^2 (\mathbf{R}_t) \otimes (\mathbf{R}_r) & \cdots & c_{N_f N_f}^2 (\mathbf{R}_t) \otimes (\mathbf{R}_r) \end{bmatrix} = \begin{bmatrix} c_{11}^2 & \cdots & c_{1N_f}^2 \\ \vdots & \ddots & \vdots \\ c_{N_f 1}^2 & \cdots & c_{N_f N_f}^2 \end{bmatrix} \otimes (\mathbf{R}_t \otimes \mathbf{R}_r). \quad (\text{C.2})$$

proof. ■

APPENDIX D NMSE DERIVATION IN (9)

The selection matrix \mathbf{S} is given by $\mathbf{S}_{\text{PCA}}(M)$, and the corresponding recovered channel is $\tilde{\mathbf{h}} = \mathbf{C}_h^{1/2} \mathbf{S}^\dagger \mathbf{S} \mathbf{a}$. Note that this is in line with the definition in (5), where the representation matrix $\mathbf{\Psi} = \mathbf{U}^H$ is the singular matrix comprising the eigenvectors of \mathbf{C}_h , and the sparse signal $\mathbf{s} = \mathbf{D}^{1/2} \mathbf{a}$ is scaled according to the diagonal singular values of \mathbf{C}_h . Thus, we can derive the NMSE as follows:

$$\begin{aligned} \delta(M) &= \text{tr} \left(\mathbb{E} \left((\mathbf{h} - \tilde{\mathbf{h}})(\mathbf{h} - \tilde{\mathbf{h}})^H \right) \right) / \text{tr} \left(\mathbb{E} \left(\mathbf{h} \mathbf{h}^H \right) \right) \\ &= \text{tr} \left(\mathbf{C}_h^{1/2} (\mathbf{I} - \mathbf{S}^\dagger \mathbf{S}) \mathbb{E}(\mathbf{a} \mathbf{a}^H) (\mathbf{I} - \mathbf{S}^\dagger \mathbf{S})^H \mathbf{C}_h^{1/2} \right) / \text{tr}(\mathbf{C}_h) \\ &= (\text{tr}(\mathbf{D}) - \text{tr}(\mathbf{SD})) / \text{tr}(\mathbf{D}). \end{aligned}$$

REFERENCES

- [1] J. Joung and S. Sun, "SCF: Sparse channel-state-information feedback using Karhunen-Loève transform," in *Proc. IEEE Global Commun. Conf. (GLOBECOM)*, Austin, TX, USA, Dec. 2014, pp. 399–404.
- [2] S. Zhou and G. B. Giannakis, "Optimal transmitter eigen-beamforming and space-time block coding based on channel mean feedback," *IEEE Trans. Signal Process.*, vol. 50, pp. 2599–2613, Oct. 2002.
- [3] Q. H. Spencer, A. L. Swindlehurst, and M. Haardt, "Zero-forcing methods for downlink spatial multiplexing in multi-user MIMO channels," *IEEE Trans. Signal Process.*, vol. 52, pp. 461–471, Feb. 2004.
- [4] L.-U. Choi and R. Murch, "A transmit preprocessing technique for multiuser MIMO systems using a decomposition approach," *IEEE Trans. Wireless Commun.*, pp. 20–24, Jan. 2004.
- [5] J. Joung, E. Y. Kim, S. H. Lim, Y.-U. Jang, W.-Y. Shin, S.-Y. Chung, J. Chun, and Y. H. Lee, "Capacity evaluation of various multiuser MIMO schemes in downlink cellular environments," in *Proc. IEEE Int. Symp. on Personal, Indoor and Mobile Radio Commun. (PIMRC)*, Helsinki, Finland, Sep. 2006.
- [6] M. Sadek, A. Tarighat, and A. H. Sayed, "A leakage-based precoding scheme for downlink multi-user MIMO channels," *IEEE Trans. Wireless Commun.*, pp. 1711–1721, May 2007.
- [7] L. Liu, R. Chen, S. Geirhofer, K. Sayana, Z. Shi, and Y. Zhou, "Downlink MIMO in LTE-advanced: SU-MIMO vs. MU-MIMO," *IEEE Commun. Mag.*, vol. 50, no. 2, pp. 140–147, Feb. 2012.
- [8] *IEEE Std 802.11n-2009*, NY, USA, IEEE Std.
- [9] *IEEE Std 802.11ac/D7.0, Sept 2013*, NY, USA, IEEE Std.
- [10] F. Verbeyst and M. Bossche, "Real-time and optimal PA characterization speeds up PA design," in *34th European Microwave Conference*, Amsterdam, Netherlands, Oct. 2004, pp. 431–434.
- [11] E. Björnson, J. Hoydis, M. Kountouris, and M. Debbah, "Massive MIMO systems with non-ideal hardware: Energy efficiency, estimation, and capacity limits." [Online]. Available: <http://arxiv.org/abs/1304.0553>
- [12] F. Rusek, D. Persson, B. K. Lau, E. G. Larsson, T. L. Marzetta, O. Edfors, and F. Tufvesson, "Scaling up MIMO: Opportunities and challenges with very large arrays," *IEEE Trans. Signal Process.*, vol. 30, pp. 40–60, Jan. 2013.
- [13] Y.-U. Jang, J. Joung, W.-Y. Shin, and E.-R. Jeong, "Frame design and throughput evaluation for practical multiuser MIMO OFDMA systems," *IEEE Trans. Veh. Technol.*, vol. 60, no. 7, pp. 3127–3141, Sep. 2011.
- [14] D. Ying, F. W. Vook, T. A. Thomas, D. J. Love, and A. Ghosh, "Kronecker product correlation model and limited feedback codebook design in a 3D channel model." [Online]. Available: <http://arxiv.org/pdf/1401.2952v1.pdf>
- [15] S. Ghosh, B. D. Rao, and J. R. Zeidler, "Outage-efficient strategies for multiuser MIMO networks with channel distribution information," *IEEE Trans. Signal Process.*, vol. 58, pp. 6312–6324, Dec. 2010.
- [16] B. Makki and T. Eriksson, "Efficient channel quality feedback signaling using transform coding and bit allocation," in *Proc. IEEE Veh. Technol. Conf. (VTC)*, Taipei, Taiwan, May 2010, pp. 1–5.
- [17] "Codebook design for 8 Tx transmission in LTE-A," Samsung, Athens, Greece, Tech. Rep. R1-090618, Feb. 2009.
- [18] S. Wagner, R. Couillet, M. Debbah, and D. Slock, "Large system analysis of linear precoding in correlated MISO broadcast channels under limited feedback," *IEEE Trans. Inf. Theory*, vol. 58, no. 7, pp. 4509–4537, Jul. 2012.
- [19] J. Joung, Y. K. Chia, and S. Sun, "Energy-efficient, large-scale distributed-antenna system (L-DAS) for multiple users," *IEEE J. Sel. Topics Signal Process.*, vol. 8, pp. 954–965, Oct. 2014.
- [20] B. Lee and B. Shim, "An efficient feedback compression for large-scale MIMO systems," in *Proc. IEEE Veh. Technol. Conf. (VTC-Spring)*, Seoul, Korea, May 2014.
- [21] B. Lee, J. Choi, J. Yun Seol, D. J. Love, and B. Shim, "Antenna grouping based feedback compression for fdd-based massive mimo systems." [Online]. Available: <http://arxiv.org/abs/1408.6009v2>
- [22] I. T. Jolliffe, *Principal Component Analysis*, 2nd ed. New York: Springer-Verlag, 1986.
- [23] M. Journée, Y. Nesterov, P. Richtárik, and R. Sepulchre, "Generalized power method for sparse principal component analysis," *J. Mach. Learn. Res.*, vol. 11, pp. 517–553, Feb. 2010.
- [24] K. Liu and C.-T. Chiu, "Unified parallel lattice structures for time-recursive discrete cosine/sine/hartley transforms," *IEEE Trans. Signal Process.*, vol. 41, pp. 1357–1377, Mar. 1993.
- [25] P.-H. Kuo, H. T. Kung, and P.-A. Ting, "Compressive sensing based channel feedback protocols for spatially-correlated massive antenna arrays," in *Proc. IEEE Wireless Commun. Netw. Conf. (WCNC)*, Paris, France, Apr. 2012, pp. 492–497.
- [26] Y. Gwon, H. T. Kung, and D. Vlah, "Compressive sensing with optimal sparsifying basis and applications in spectrum sensing," in *Proc. IEEE Global Commun. Conf. (GLOBECOM)*, Anaheim, CA, USA, Dec. 2012, pp. 5386–5391.
- [27] E. Kurniawan, J. Joung, and S. Sun, "Limited feedback scheme for massive MIMO in mobile multiuser FDD systems," in *Proc. IEEE Int. Conf. Commun. (ICC)*, London, UK, Jun. 2015.
- [28] E. J. Candès, J. Romberg, and T. Tao, "Robust uncertainty principles: Exact signal reconstruction from highly incomplete frequency information," *IEEE Trans. Inf. Theory*, vol. 52, no. 2, pp. 489–509, Feb. 2006.
- [29] R. Masiero, G. Quer, D. Munaretto, M. Rossi, J. Widmer, and M. Zorzi, "Data acquisition through joint compressive sensing and principal component analysis," in *Proc. IEEE Global Commun. Conf. (GLOBECOM)*, Honolulu, Hawaii, USA, Dec. 2009, pp. 1–6.
- [30] Y. Hua and W. Liu, "Generalized Karhunen-Loève transform," *IEEE Signal Process. Lett.*, vol. 5, no. 6, pp. 141–142, Jun. 1998.
- [31] J. P. Kermoal, L. Schumacher, K. I. Pedersen, P. E. Mogensen, and F. Frederiksen, "A stochastic MIMO radio channel model with experimental validation," *IEEE J. Sel. Areas Commun.*, vol. 20, pp. 1211–1226, Aug. 2002.
- [32] A. Adhikary, J. Nam, J. Y. Ahn, and G. Caire, "Joint spatial division and multiplexing—The large-scale array regime," *IEEE Trans. Inf. Theory*, vol. 59, no. 10, pp. 6441–6463, Oct. 2013.
- [33] J. G. Proakis and M. Salehi, *Digital communications*, five ed. New York: McGraw-Hill, 2007.
- [34] T. Matsumoto, Y. Hatakawa, and S. Konishi, "Experimental performance evaluation of time-domain CSI compression scheme for multiuser MIMO," in *Proc. IEEE Asia Pacific Wireless Communications Symposium (APWCS)*, Seoul, Korea, Aug. 2013, pp. 327–331.
- [35] C. d. Boor, *A Practical Guide to Splines*, revised ed., ser. Applied Mathematical Sciences. New York: Springer-Verlag, 2001.